The effect of noise on a hyperbolic strange attractor in the system of two coupled van der Pol oscillators

Alexey Yu. Jalnine, Sergey P. Kuznetsov

May 1, 2008

Saratov Branch of Institute of Radio-Engineering and Electronics, Russian Academy of Sciences, Zelenaya 38, Saratov, 410019, Russia

Abstract

We study the effect of noise for a physically realizable flow system with a hyperbolic chaotic attractor of the Smale - Williams type in the Poincaré cross-section [S.P. Kuznetsov, Phys. Rev. Lett. 95, 2005, 144101]. It is shown numerically that slightly varying the initial conditions on the attractor one can obtain a uniform approximation of a noisy orbit by the trajectory of the system without noise, that is called as the "shadowing" trajectory. We propose an algorithm for locating the shadowing trajectories in the system under consideration. Using this algorithm, we show that the mean distance between a noisy orbit and the approximating one does not depend essentially on the length of the time interval of observation, but only on the noise intensity. This dependance is nearly linear in a wide interval of the intensities of noise. It is found out that for weak noise the Lyapunov exponents do not depend noticeably on the noise intensity. However, in the case of a strong noise the largest Lyapunov exponent decreases and even becomes negative indicating the suppression of chaos by the external noise.

One of the intensively studied problems in nonlinear science is the investigation of the effect of noise for the systems with complex dynamical behavior, in particular for the ones possessing strange chaotic attractors. It is known that strange attractors in finite-dimensional nonlinear systems can be subdivided into three main classes: uniformly hyperbolic, non-uniformly hyperbolic (quasi-hyperbolic) and non-hyperbolic [1, 2, 3, 4, 5]. Effects of noise on attractors of these classes have some specific features [2].

The objects referred to as non-hyperbolic attractors, or quasiattractors, are not well defined. They are composed of a set of complex orbits including chaotic limit sets and stable periodic orbits with extremely narrow basins of attraction. In this case, the presence of external noise appears as a saving remedy for using the tools of the nonlinear dynamics based on existence of a definite unique probabilistic measure. Thus, in principle, the account of noise is of crucial significance for non-hyperbolic attractors. For hyperbolic attractors the effect of noise is not so essential because their intrinsic chaotic properties are sufficient to ensure legitimacy of the description in terms of a natural invariant measure. This statement is validated rigorously on a solid axiomatic basis for the uniform hyperbolic attractors (the so-called SRB measures by Sinai, Ruelle, and Bowen [1, 2, 3, 4, 5, 6]). It is known that the SRB

measures correspond to zero-noise-limit. It means that they serve as a good approximation for the systems under a weak noise as well [6, 7]. Moreover, a strong result may be formulated in concern to individual orbits basing on the so-called shadowing lemma [5, 8, 9, 10, 11]. Namely, on a time interval of duration as long as wished, any motion of the system with weak noise in the sustained regime may be represented approximately by an orbit on the attractor of the system without noise. In this sense, the noise may be regarded as unessential at all! As for the non-uniform hyperbolic attractors, for conditions of existence of invariant measures and for shadowing properties of orbits, we refer a reader to a vast recent literature (see [4] and references therein).

Formally, the understanding the effect of noise seems to be in the clearest state for the uniformly hyperbolic attractors, but, in fact, it is not yet a state that can satisfy a physicist. Indeed, no physical examples of the uniformly hyperbolic attractors have been known until recent time. For this reason, the formulation of the problem in the physical aspect was not possible till now.

An idea of implementation of a kind of a uniformly hyperbolic attractor was advanced in Ref. [12] in application to a system of two coupled non-autonomous van der Pol oscillators. In the Poincaré map of this system a chaotic attractor has been found similar to the Smale - Williams solenoid. An analogous system has been built as an electronic device and studied in experiment [13]. Numerical verification of conditions for a theorem guaranteeing the hyperbolicity was performed in Ref. [14]. Some other examples of complex dynamics were discussed in Refs. [15, 16, 17, 18] basing on the same idea.

In the current article we report some results concerning the effect of white Gaussian noise on the system of alternately excited non-autonomous oscillators [12]. We discuss the numerical simulation of the dynamics in the presence of noise and present an algorithm for locating the shadowing trajectories, which reproduce with a certain accuracy the orbits of the noisy system. The algorithm is based on a step-by-step approach to the noisy orbits and it gives a uniform approximation with a mean deviation not depending upon the length of the time interval. We demonstrate numerically that for the weak noise the magnitude of the deviation from the noisy orbit remains small and it tends to zero linearly with the decrease of the noise intensity. Additionally, we analyze a dependence of the Lyapunov exponents on the noise level. At weak noise they do not depend noticeably on the noise intensity. This result agrees well with the assertion that the SRB measure corresponds to the zero-noise limit of the probabilistic measure. For strong noise, the largest Lyapunov exponent decreases. It can become even negative indicating the suppression of chaos by the external noise.

We study the model system determined by the following equations:

$$\begin{aligned} &\ddot{x} - [A\cos(\omega_0 t/N) - x^2]\dot{x} + \omega_0^2 x = \varepsilon y \cos\omega_0 t + D_1\xi(t), \\ &\ddot{y} - [-A\cos(\omega_0 t/N) - y^2]\dot{y} + 4\omega_0^2 y = \varepsilon x^2 + D_2\xi(t). \end{aligned} \tag{1}$$

It is a pair of coupled non-autonomous van der Pol oscillators with basic frequencies ω_0 and $2\omega_0$. The control parameters in both subsystems slowly vary periodically in time in counter-phase ($\pm A\cos(\omega_0 t/N)$), and some special type of coupling between the subsystems is introduced. The frequency ratio N is assumed to be an integer. A turn-by-turn transfer of excitation between the subsystems is accompanied with a transformation of the phase at successive periods of modulation governed by the expanding circle map, or Bernoulli map: $\varphi_{n+1} = 2\varphi_n + const \pmod{2\pi}$. The gaussian white noise $\xi(t)$ with $\langle\xi(t)\rangle = 0$ and $\langle\xi(t)\xi(t-\tau)\rangle = \delta(\tau)$ is added to the right-hand parts of the equations. Parameters $D_{1,2}$ characterizing the noise intensity can be varied in a wide range.

As argued in the previous studies [12, 13, 14], the Poincaré map of the noiseless system defined for a period of the external driving $T = 2\pi N/\omega_0$ possesses a uniformly hyperbolic chaotic attractor, namely, a Smale - Williams solenoid embedded in the four-dimensional phase space.

For numerical solution of the stochastic equations (1) we exploit a second-order order method described in Ref. [19]. A plot in Fig. 1(a) shows the results of computation for the noisy system at the parameters $A = 3.0, \varepsilon = 0.5, \omega_0 = 2\pi, N = 10$ and at the noise intensity $D_1 = D_2 = 0.02$. In gray color we show 100 superimposed samples of the process under effect of noise started from identical initial conditions. Due to the noise, in the final part of the interval of observation the states appear to be essentially different because of instability intrinsic to the orbits on the chaotic attractor. As the result, the picture becomes fuzzy. For comparison, the curve shown in black color is related to the system without noise, started from the same initial conditions.

It is easy to demonstrate qualitatively that a very similar picture is observed in the noiseless system if one considers an ensemble of samples with a slight deviation of the initial conditions. In Fig. 1(b) we show a set of 100 samples for the system without noise launched from initial conditions with a small random variation near the same initial state as in the previous diagram. The range of the random variations is specially selected to obtain close degree of mutual divergence of the orbits on the considered time interval in comparison with that produced by the effect of noise.

As shown for the noiseless system, the phases determined at successive stages of activity for one of the subsystems obey approximately the Bernoulli map. It is interesting to investigate the influence of noise on the iteration diagrams for phases. Such diagrams were used in Refs. [12, 13, 14, 15] for substantiation of the classification of the attractors as the hyperbolic ones. Taking into account that during the active stage the oscillations of $x(t)$ are close to sinusoidal ones with modulated amplitude and floating phase ($x(t) \sim \cos(\omega_0 t + \varphi)$, see Ref. [12]), let us determine the phase at the time moments $t_n = t_0 + nT$ as follows:

$$\varphi_n = \arg[\dot{x}(t_n) + i\omega_0 x(t_n)].$$

Figure 2 shows the iteration diagrams for the phases in presence of noise (gray) and without noise (black). Note, that the presence of noise of sufficiently low intensity does not change the topological nature of the phase map, which remains in the same class as the Bernoulli map $\varphi_{n+1} = 2\varphi_n + const \pmod{2\pi}$.

Another approach that allows us to compare the noisy and the noiseless dynamics is based on the analysis of the Lyapunov exponents. For our model they can be computed from the linearized equations

$$\begin{aligned} &\ddot{\tilde{x}} - [A\cos(\omega_0 t/N) - x^2]\dot{\tilde{x}} + (2x\dot{x} + \omega_0^2)\tilde{x} = \varepsilon\tilde{y}\cos\omega_0 t, \\ &\ddot{\tilde{y}} + [A\cos(\omega_0 t/N) + y^2]\dot{\tilde{y}} + (2y\dot{y} + 4\omega_0^2)\tilde{y} = 2\varepsilon x\tilde{x}, \end{aligned} \tag{2}$$

where tilde designates small perturbations of the dynamical variables. These equations have to be solved numerically together with the stochastic equations (1). To obtain the spectrum of all the four Lyapunov exponents we consider a set of four perturbation vectors $(\tilde{x}, \dot{\tilde{x}}/\omega_0, \tilde{y}, \dot{\tilde{y}}/2\omega_0)$ and apply the procedure of Gram - Schmidt orthogonalization after each period of the parameter modulation. In Fig. 3 the Lyapunov exponents are plotted versus the noise intensity parameter $D = D_1 = D_2$. At small intensities of noise, the largest Lyapunov exponent is close to the value of $T^{-1}\ln 2$, which corresponds to the approximate

description of the dynamics by the Bernoulli map. A notable deflection appears only at a sufficiently high level of noise, namely, at $D \geq 0.2$. At $D \sim 0.5$ the effect of noise is already very relevant, the largest Lyapunov exponent crosses zero and becomes negative indicating the suppression of the intrinsic dynamical chaos by the external noise. Dependence of other Lyapunov exponents on the noise intensity is not noticeable at all.

Now we turn to the main part of the present paper. Namely, we are going to illustrate numerically that in our model with a hyperbolic attractor the weak noise is indeed non-essential, i.e., a typical noisy orbit can be reproduced for a long time interval by a trajectory without noise due to a careful appropriate choice of the initial conditions. This statement follows mathematically from the hyperbolic nature of the attractor and is based on the applicability of the shadowing lemma.

Suppose two trajectories are launched form identical initial conditions, one in the "pure" system without noise and another one in the system with noise. Obviously, the "noisy" orbit will diverge from the "pure" one. Now, let us try to vary the initial conditions for the pure trajectory to get an approximation for the noisy orbit in the best way at a long time interval. The whole construction is performed for a definite sample of the noisy orbit obtained with the same sample of noise.

To explain the method of selection of the initial conditions, it seems appropriate to consider the Poincaré map produced by a period-T stroboscopic section of the flow system (1) without noise. Let us suppose that we have an instantaneous state given by a vector $\mathbf{V}_n = (x, \dot{x}/\omega_0, y, \dot{y}/2\omega_0)$ at $t_n = t_0 + nT$. Then, after the time interval T we have a new state

$$\mathbf{V}_{n+1} = \hat{\mathbf{F}}_{t_0}(\mathbf{V}_n). \tag{3}$$

In practice, such map can be obtained from numerical integration of the system (1) with $D_1 = D_2 = 0$. In Fig. 4(a) one can see a portrait of the attractor of the map projected onto the plane $(x, \dot{x}/\omega_0)$. The attractor manifests filaments of an infinite number of wraps possessing the Cantor-like structure in the cross-section. Solid black dots in the picture denote four successive points of the stroboscopic section of one specially chosen trajectory on the attractor. The black line passing through each dot designates the respective unstable direction $\mathbf{D}^u$, which is tangent to the unstable manifold W^u at the given point. These directions can be simply approximated numerically from long-time evolution of an arbitrarily chosen unit perturbation vector $\tilde{\mathbf{V}}_n = (\tilde{x}, \dot{\tilde{x}}/\omega_0, \tilde{y}, \dot{\tilde{y}}/2\omega_0)$ at $t_n = t_0 + nT$, since such a vector governed by the linearized system (2) tends to the unstable direction associated with a single positive Lyapunov exponent.

Now one should take a note of how a cloud of representative points evolves from the same initial conditions in the presence of noise. An illustration is shown in Fig. 4(b). The dots pictured in gray are obtained in the Poincaré cross-section, i.e., stroboscopically at each next period T from 10^4 sample orbits of the noisy system at $D_1 = D_2 = 0.02$. The black dots correspond to the trajectory of the system without noise ($D_1 = D_2 = 0$) launched from the same initial conditions. Note, that the cloud stretches along the unstable direction tangent to the filaments forming the attractor, but it does not grow in the radial direction.

The algorithm for localization of the "pure" trajectory, which approximates a noisy orbit, consists in the following. Let us denote the original noisy orbit as $\mathbf{V}_{noisy}(t)$, while the pure trajectory in zero approximation is denoted as $\mathbf{V}^{(0)}(t)$. We start first from the initial conditions at $t = t_0$ identical for the noisy and the pure orbit: $\mathbf{V}_{noisy}(t_0) = \mathbf{V}^{(0)}(t_0)$. The starting point is supposed to belong to the attractor of the system without noise. Then, computing the two trajectories $\mathbf{V}_{noisy}(t)$ and $\mathbf{V}^{(0)}(t)$, we consider the norm of the difference

vector $\| \Delta\mathbf{V}^{(0)}(t_1) \| = \| \mathbf{V}_{noisy}(t_1) - \mathbf{V}^{(0)}(t_1) \|$ at the time moment $t_1 = t_0 + T$. Next, we slightly modify the initial condition for the pure orbit from $\mathbf{V}^{(0)}(t_0)$ to $\mathbf{V}^{(1)}(t_0)$ with the purpose to minimize the norm of the difference $\| \mathbf{V}_{noisy}(t_1) - \mathbf{V}^{(1)}(t_1) \|$. It is done by variation of the phase of the partial oscillator active at the time moment $t = t_0$. For our system it corresponds to variation of the initial state along the unstable direction associated with the point on the attractor, or, that is the same, along a filament of the attractor containing the initial point.

In detail the procedure of the search for new initial conditions $\mathbf{V}^{(1)}(t_0)$ looks as follows. We define a set of $2m+1$ initial conditions stretched along the unstable direction $\mathbf{V}_{1,k}(t_0) = \mathbf{V}^{(0)}(t_0) + \Delta V^{(1)}(k/m)\mathbf{D}^u$, where $k = -m, \ldots, m$, $\| \mathbf{D}^u \| = 1$, and the maximum variation is chosen from the relation $\Delta V^{(1)} = \| \Delta\mathbf{V}^{(0)}(t_1) \| \exp(-\lambda_1 T)$. We trace then $2m+1$ trajectories till $t = t_1$ and choose the one at some $k = k_1$, which minimizes the error $\| \mathbf{V}_{noisy}(t_1) - \mathbf{V}_{1,k_1}(t_1) \|$. This trajectory is denoted as $\mathbf{V}_1^{(1)} = \mathbf{V}_{1,k_1}$. Next, we redefine the set of $2m+1$ initial conditions as $\mathbf{V}_{2,k}(t_0) = \mathbf{V}_1^{(1)}(t_0) + \Delta V^{(1)}(k/m^2)\mathbf{D}^u$ and select the trajectory, which minimizes the error $\| \mathbf{V}_{noisy}(t_1) - \mathbf{V}_{2,k_2}(t_1) \|$ at $k = k_2$. It is the trajectory $\mathbf{V}_2^{(1)} = \mathbf{V}_{k_2}$. We repeat this procedure of successive adjustment of the initial conditions again and again obtaining a sequence of the initial conditions $\{\mathbf{V}_l^{(1)}(t_0)\}_{l=1,2,\ldots}$ and estimate the limit $\mathbf{V}^{(1)}(t_0)$. In computations, the procedure is stopped after a sufficiently large number of steps, when further increase of accuracy does not result in a decrease of the final deviation of the pure trajectory from the noisy one at $t = t_1$.

Suppose we take a new initial condition for the pure orbit $\mathbf{V}^{(1)}(t_0)$. Now with the same sample of the noise we again trace two trajectories, the noisy one starting from $\mathbf{V}_{noise}(t_0)$ and the pure one starting from $\mathbf{V}^{(1)}(t_0)$ for a longer time interval up to $t_2 = t_0 + 2T$, and obtain the norm of the difference vector $\| \Delta\mathbf{V}^{(1)}(t_2) \| = \| \mathbf{V}_{noisy}(t_2) - \mathbf{V}^{(1)}(t_2) \|$. Then, modifying again the initial condition for the pure orbit by variation of the initial phase of the active oscillator, at this time in closer neighborhood of $\mathbf{V}^{(1)}(t_0)$, we try to minimize $\| \mathbf{V}_{noisy}(t_2) - \mathbf{V}^{(2)}(t_2) \|$ and obtain the new initial condition $\mathbf{V}^{(2)}(t_0)$. The procedure of variation of the initial conditions is the same as the described above with the only difference that the maximum variation $\Delta V^{(2)}$ is chosen from the relation of $\Delta V^{(2)} = \| \Delta\mathbf{V}^{(1)}(t_2) \| \exp(-2\lambda_1 T)$. Step by step we successively increase the time interval nT and select the initial conditions for the pure orbit $\mathbf{V}^{(n)}(t_0)$, which deliver minimal values for the norms of the differences $\| \mathbf{V}_{noisy}(t_n) - \mathbf{V}^{(n)}(t_n) \|$. Note, that the maximum variation of the initial condition at the n-th step of the algorithm decays as $\Delta V^{(n)} \sim \exp(-n\lambda_1 T)$. Due to the recurrent nature of the algorithm, it appears that the approximation of the noisy orbit by the pure one holds uniformly along the whole time interval $[t_0, t_0 + nT]$.

Figure 5 illustrates results of application of several steps of the above algorithm. Parameters of the system are taken the same as those in the previous examples of computations, and the noise intensity is $D_1 = D_2 = 0.1$.

The first plot in Fig. 5 corresponds to the initial step of the algorithm: the noisy (gray) and pure (black) trajectories start from identical initial conditions. One can see their sufficiently fast divergence: the phase synchronism disappears already after one period of the parameter modulation T. After the first modification of the initial conditions for the pure orbit the divergence is delayed and the phase synchronism persists over $1-2$ periods of T, but then the orbits diverge. At the next steps of the algorithm the time intervals of existence of the phase synchronism become longer and longer and occupy finally the whole range in the diagram. Figure 6 shows in gray color 20 dots of the projection of the noisy

orbit at $D_1 = D_2 = 0.04$ on the $(x, \dot{x}/\omega_0)$ plane. In black color 20 dots are shown in the same stroboscopic cross-section of the approximating pure trajectory recovered by the above method.

To characterize the degree of closeness of a noisy orbit to a shadowing pure orbit, we use the following value

$$\rho_k = \frac{1}{kT} \int_{t_0}^{t_0+kT} \parallel \mathbf{V}_{noisy}(t) - \mathbf{V}^{(k)}(t) \parallel dt,$$

where k designates the duration of the considered time interval in units of the modulation period T. Averaging this quantity over an ensemble of initial conditions and noise samples we obtain a mean deviation $\langle \rho_k \rangle$, characterizing the degree of closeness of the noisy and shadowing trajectories on the attractor. In Fig. 7(a) we present plots of the mean deviation $\langle \rho_k \rangle$ versus the value of k for different noise levels. It can be seen in the figure that the mean deviation depends on k very weakly in the range $k = 8 \ldots 50$. At $k \sim 50 - 60$ the errors become noticeable due to the finite-digital arithmetic and for the considered level of accuracy further observation of the shadowing becomes impossible.

Figure 7(b) shows a plot of the mean deviation $\langle \rho_k \rangle$ computed for $k = 9$ in dependence on the parameter of the noise intensity $D = D_1 = D_2$. For each D value we consider a set of 100 orbits launched from different initial conditions and calculated for different noise series. Each noisy orbit was approximated by the shadowing one with the method described above, and the mean value $\langle \rho_9 \rangle$ was obtained over the set of orbits. As seen from the figure, the dependence $\langle \rho_9 \rangle$ versus D looks like a linear one in the range of D from zero to 0.1.

In this article we have examined the effect of Gaussian noise on a physically realizable system with a uniformly hyperbolic attractor. In the context of the shadowing lemma known from the mathematical literature, one could expect that in our model the effect of weak noise can be compensated by a careful selection of initial conditions. We developed the numerical algorithm that allows one to locate the shadowing trajectories of the noiseless system and provide a uniform approximation of orbits of the noisy system. Using this algorithm, we have demonstrated numerically that the mean mutual deviation between the noisy orbit and the noiseless shadowing trajectory does not depend noticeably on the length of the considered time interval, but depends on the intensity of noise. This dependence was shown to be almost linear in a sufficiently wide range of the parameter D variation. As well, we have demonstrated that the weak noise does not change the nature of the chaotic phase dynamics. Similarly, the weak noise does not change noticeably the Lyapunov exponents characterizing quantitatively the degree of instability of the motion. At larger intensities the noise can suppress the intrinsic chaotic dynamics of the system, and the largest Lyapunov exponent becomes negative.

The authors thank Dr. D.S. Goldobin for useful discussions and Dr. M.D. Prokhorov for assistance in preparation of the paper. We acknowledge support from the RFBR - DFG grant No. 04-02-04011.

References

[1] L.P. Shilnikov, A.L. Shilnikov, D.V. Turaev, and L.O. Chua. *Methods of Qualitative Theory in Nonlinear Dynamics*, parts I and II (World Scientific, Singapore, 1998 and 2002).

[2] V.S. Anishchenko, T.E. Vadivasova, G.A. Okrokvertskhov, G.I. Strelkova. Physics Uspekhi **48**(2), 151-166 (2005).

[3] A. Katok and B. Hasselblatt. *Introduction to the Modern Theory of Dynamical Systems* (Cambridge: Cambridge University Press, 1995).

[4] L.J. Diaz, M. Viana. *Dynamics Beyond Uniform Hyperbolicity. A Global Geometric and Probabilistic Perspective* (Springer: Berlin, Heidelberg, New York, 2005, 390p.).

[5] J. Guckenheimer and P. Holmes. *Nonlinear Oscillations, Dynamical Systems, and Bifurcations of Vector Fields* (Springer, 2002, 480p.).

[6] L.-S. Young. J. Stat. Physics, **108**(5-6), 733-754 (2002).

[7] J.I. Kifer. Math. USSR Izv., **8**(5), 1083-1107 (1974).

[8] J.D. Farmer and J.J. Sidorowich. Physica D, **47**, 373-392 (1991).

[9] R. Bowen. Amer. J. Math., **92**, 725-747 (1970).

[10] Y.-C. Lai, Z. Liu, G.-W. Wei, C.-H. Lai. Phys. Rev. Lett., **89**, 184101 (2002).

[11] V.S. Anishchenko, A.S. Kopeikin, T.E. Vadivasova, G.I. Strelkova, J. Kurths. Phys. Rev. E, **62**, 7886-7893 (2000).

[12] S.P.Kuznetsov. Phys. Rev. Lett., **95**, 144101 (2005).

[13] S.P.Kuznetsov, E.P.Seleznev. JETP, **102**(2), 355-364 (2006).

[14] S.P. Kuznetsov and I.R. Sataev. Phys. Lett. A, **365**(1-2), 97-104 (2007).

[15] S.P. Kuznetsov and A. Pikovsky. Physica D, **232**, 87-102 (2007).

[16] O.B.Isaeva, A.Yu. Jalnine and S.P.Kuznetsov. Phys. Rev. E, **74**, 046207 (2006).

[17] A.Yu. Jalnine and S.P. Kuznetsov. Technical Physics, **52**(4), 401-408 (2007).

[18] O.B. Isaeva, S.P. Kuznetsov and A.H. Osbaldestin. Tech. Phys. Lett., **33**(9), 748-751 (2007).

[19] R. Mannella, V. Palleschi. Phys. Rev. A, **40**, 3381-3386 (1989).

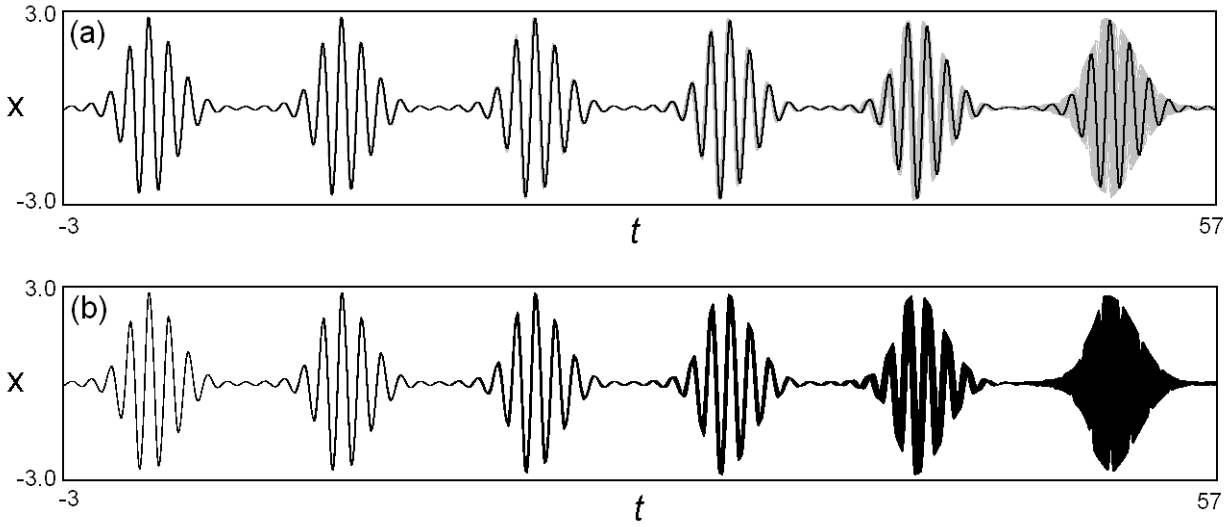

Figure 1: Temporal realizations of the variable x of the model (1): (a) superimposed 100 samples obtained at the noise level $D_1 = D_2 = 0.02$ (gray) and the trajectory without noise (black), all with the same initial conditions; (b) superimposed 100 samples for the system without noise ($D_1 = D_2 = 0$) for the ensemble of slightly different initial conditions. Here and thereafter the parameters of the system (1) are chosen to be $A = 3.0, \varepsilon = 0.5, \omega_0 = 2\pi$, and $N = 10$.

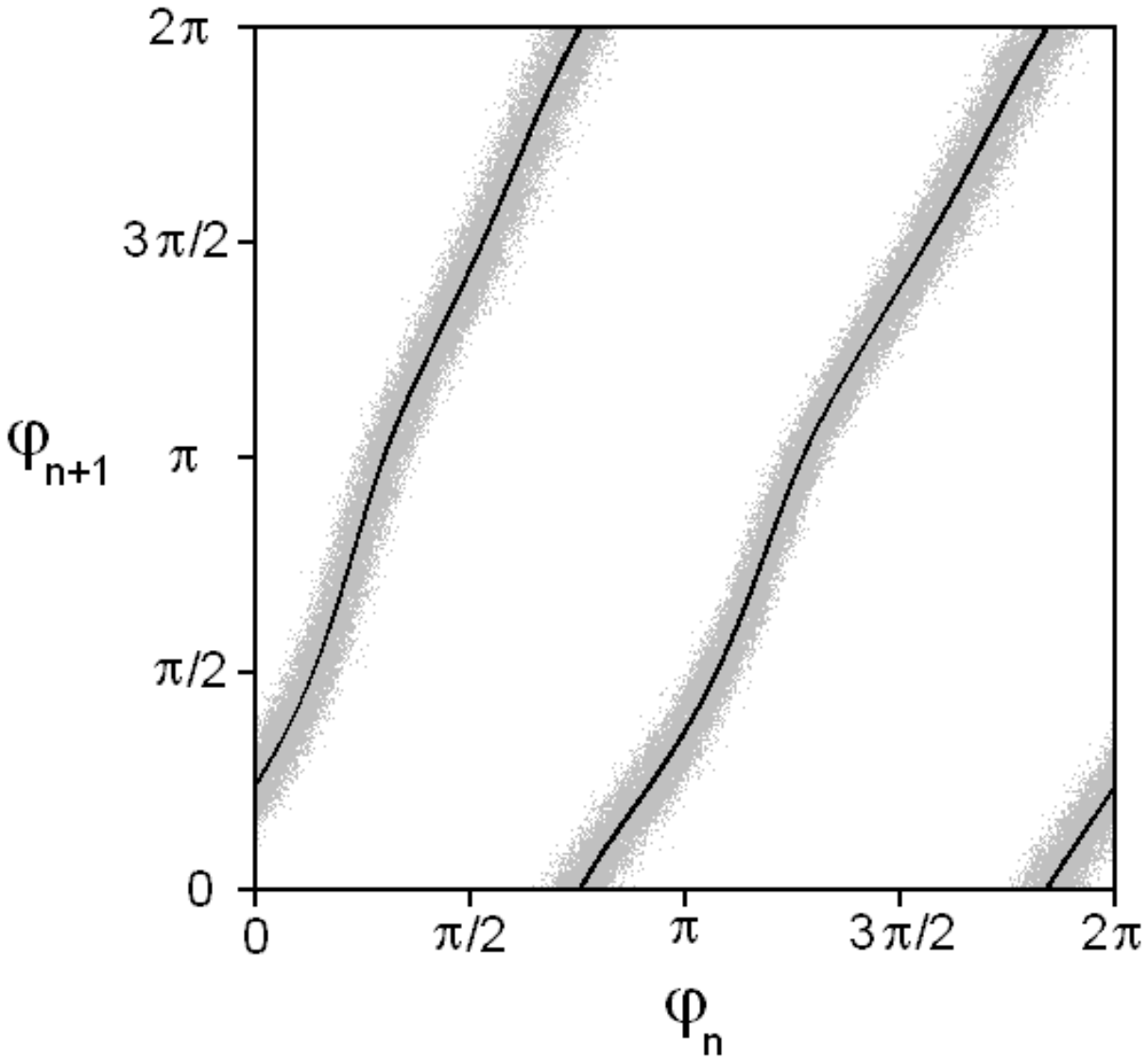

Figure 2: Iteration diagrams for the phase of the first subsystem of the model (1) with noise $D_1 = D_2 = 0.1$.

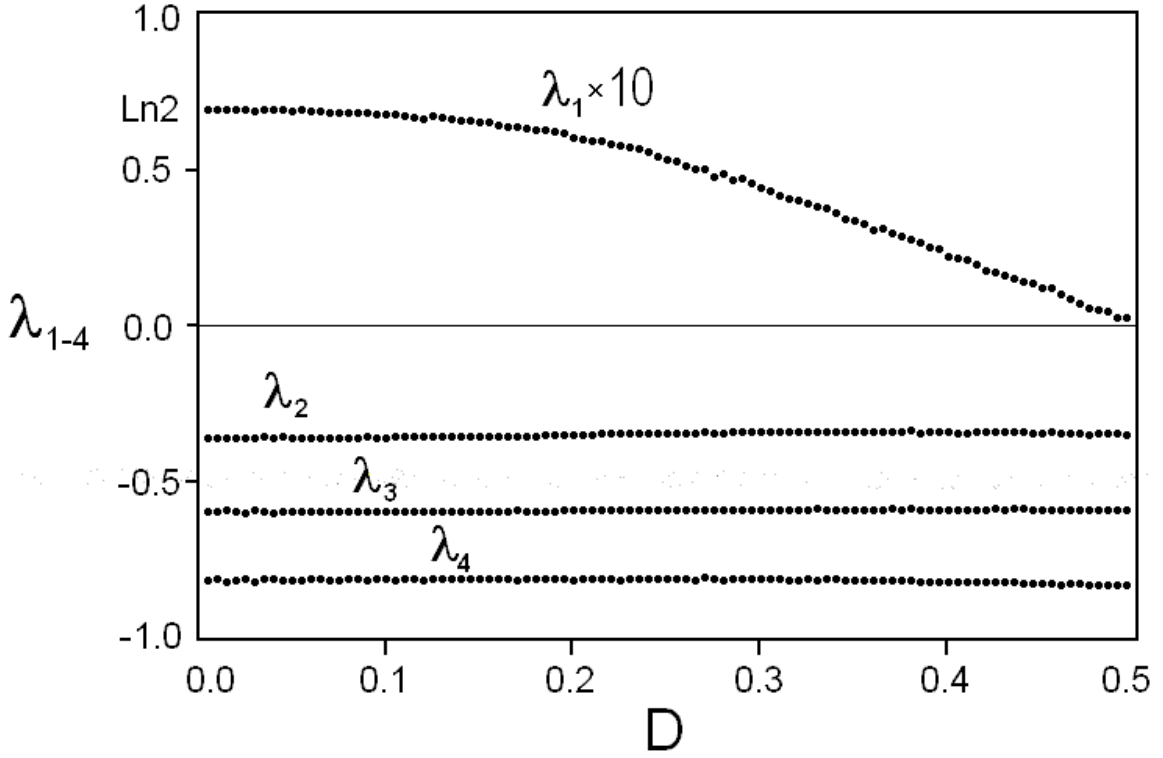

Figure 3: Spectrum of the Lyapunov exponents versus intensity of noise for the model (1) with $D_1 = D_2 = D$.

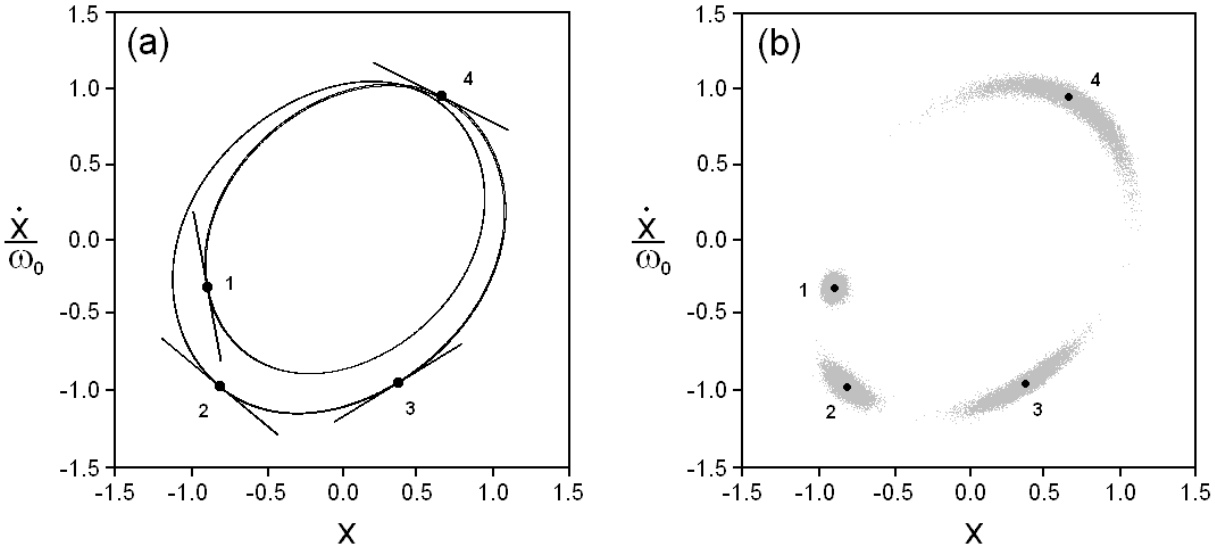

Figure 4: (a) The stroboscopic cross-section of the attractor of the system (1) at $t_0 = 0.0$. The attractor is projected on the phase plane of the first subsystem. (b) Evolution of the cloud of representative points launched from identical initial conditions in the presence of noise ($D_1 = D_2 = 0.02$). The figures $1 \ldots 4$ indicate the number of steps of the Poincaré map. An ensemble of 10^4 orbits is shown. Black dots correspond to the system without noise starting from the same initial conditions.

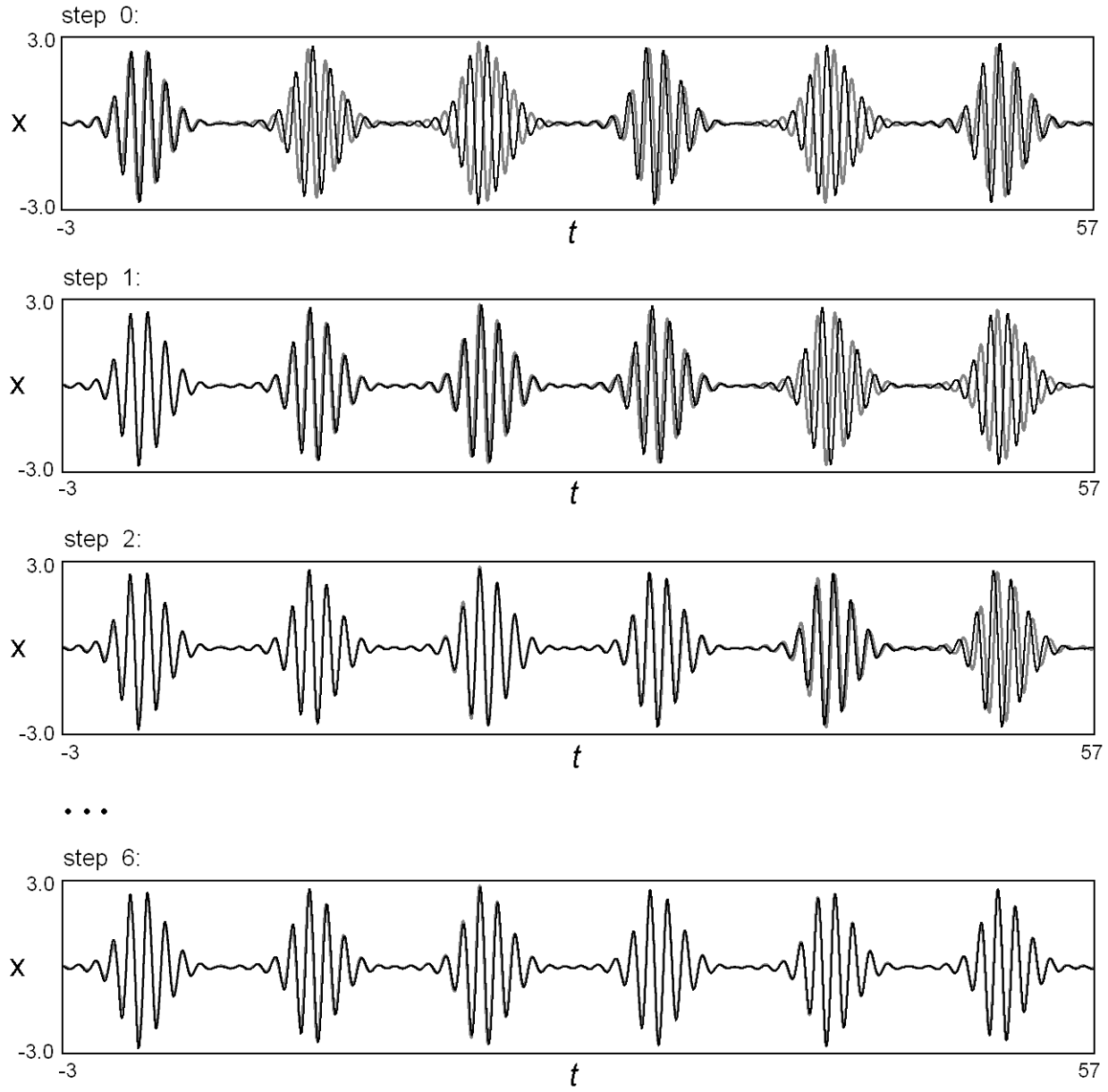

Figure 5: Successive steps of constructing the shadowing trajectory (black) to the given noisy orbits (gray). At the initial step both orbits start from the identical initial conditions. At the last presented diagram the shadowing takes place over the time range of six modulation periods.

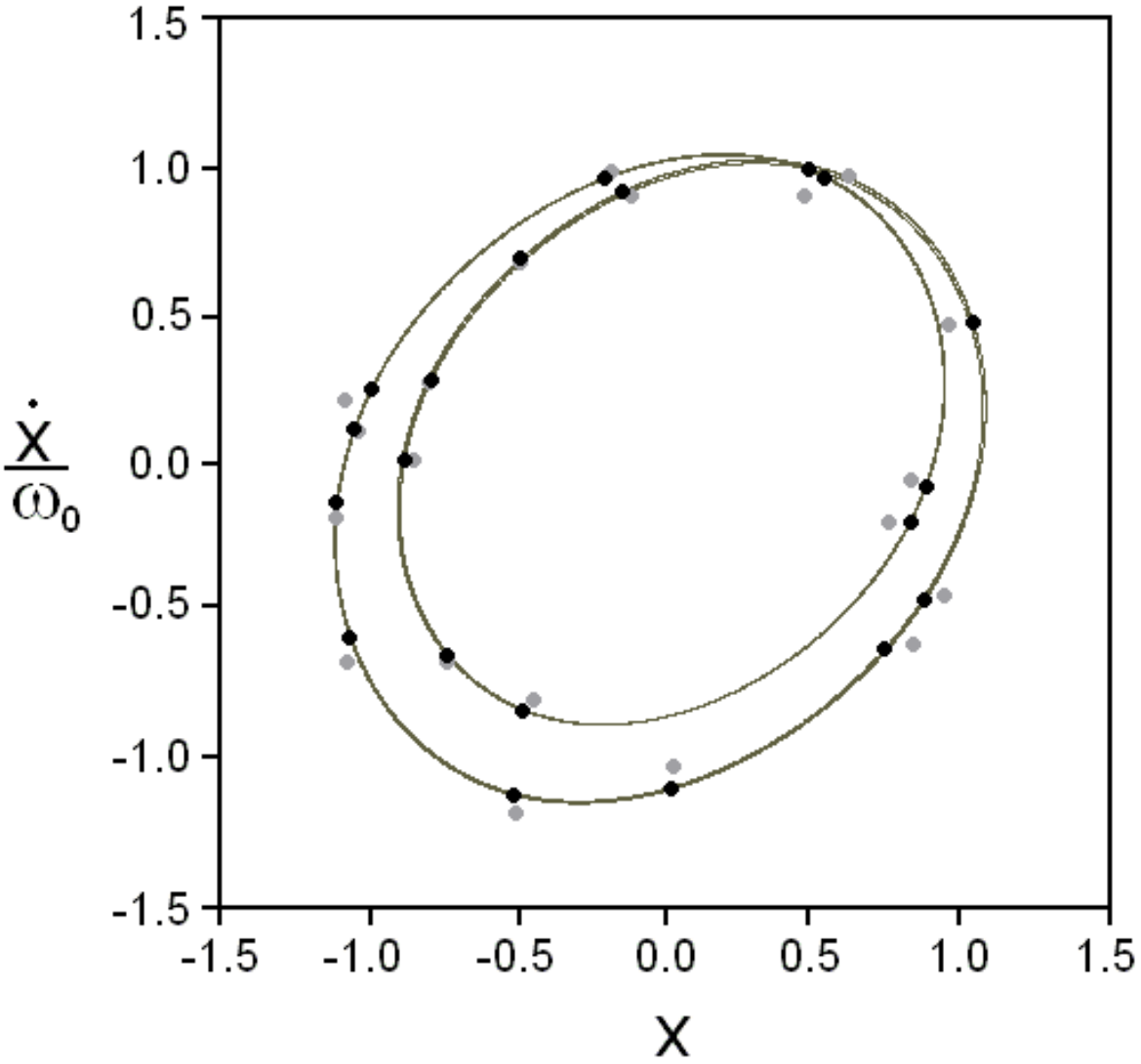

Figure 6: Stroboscopic cross-section of the noisy (light gray) and the shadowing noiseless (black) trajectories on a background of the attractor (dark gray). The trajectories are projected onto the phase plane of the first subsystem. The noise intensity $D_1 = D_2 = 0.04$.

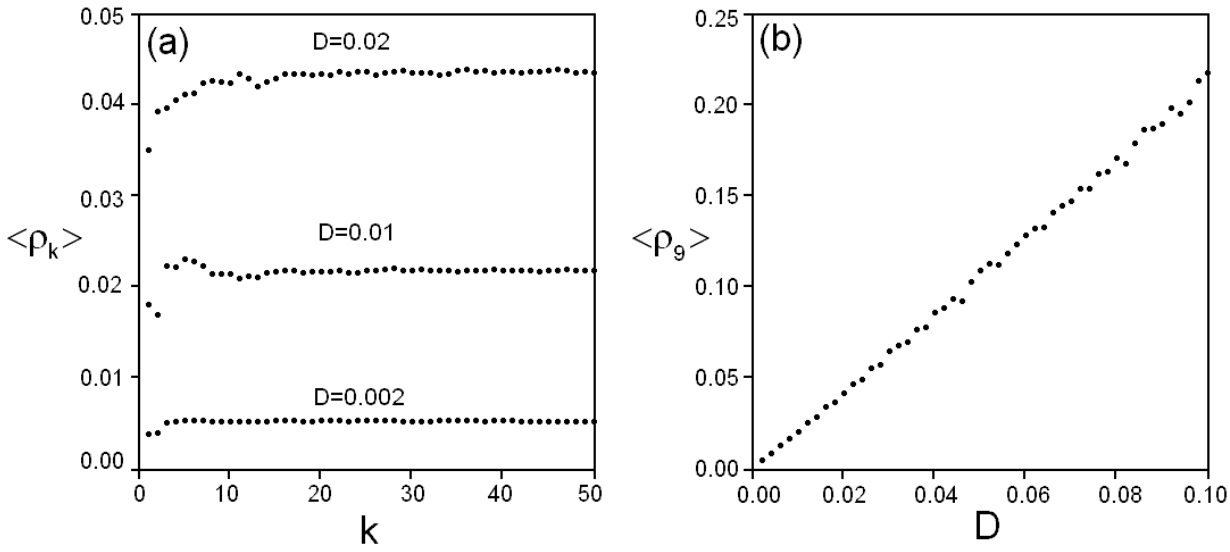

Figure 7: (a) Mean average mutual deviation of noise and shadowing trajectories $\langle \rho_k \rangle$ versus the number of modulation periods taken for the computations at the three noise levels $D_1 = D_2 = 0.002$, 0.01 and 0.02. (b) The dependence of $\langle \rho_k \rangle$ on the noise intensity D for $k = 9$.